ChemComm

COMMUNICATION

View Article Online
View Journal | View Issue

Cite this: *Chem. Commun.*, 2022, 58, 8133

Received 27th April 2022,
Accepted 22nd June 2022

DOI: 10.1039/d2cc02383k

rsc.li/chemcomm

Building-block exchange synthesis of amino-based three-dimensional covalent organic frameworks for gas chromatographic separation of isomers†

Hai-Long Qian, *[abc] Zi-Han Wang,[c] Jing Yang[c] and Xiu-Ping Yan [acd]

Thermally stable three-dimensional covalent organic frameworks (3D COFs) with rich pores of channels and cages are promising as stationary phases for gas chromatography (GC), which has not been explored. Here we synthesize the first amino-based 3D COF and its covalently bonded capillary *via* building-block exchange for GC separation of isomers.

COFs have drawn much attention owing to their pre-designable ordered structures with permeant pores and remarkable applications in energy storage, catalysis, sensing and separation.[1–3] Planar monomers covalently form long-range atomic layers that further stack into crystalline two-dimensional (2D) COFs *via* non-covalent interaction including π–π stacking and hydrogen bonding. Tetrahedral monomers tend to form 3D COFs with complete covalent bonds.[4,5] 3D COFs with richer pores of channels and cages than 2D COFs facilitate the host–guest interaction and the complete covalent bonds make 3D COFs thermally stable, endowing them with more advantages as the stationary phase (SP) for gas chromatography (GC).[6] Recently, 2D COFs have been applied as the SP for GC and great separation performance has been achieved.[7–10] However, the potential of 3D COFs for GC has not been explored yet.

Separation of petrochemical isomers is of great concern for industry and the environment, but remains challenging owing to their similar properties.[11,12] For example, *p*-xylene is the indispensable feedstock for polyethylene terephthalate, but *o*-xylene, *m*-xylene and ethylbenzene with similar sizes, boiling points and polarizabilities always exist as impurities in *p*-xylene, increasing the challenge of their separation and quantitation.[13,14] A lot of novel SPs for GC have been developed for the separation of petrochemical isomers,[8,9,15–17] but the baseline separation of isomers especially xylene isomers by a facile process has been rarely realized.

The separation by GC largely depends on the non-covalent interaction of the SP with analytes. Introducing functional groups with diverse interactions plays a key role in promoting the capabilities of SPs.[18,19] Thus, the versatile polar amino functionalized 3D COF, 3D COF-NH_2, intends to be a promising SP.[20,21] However, the involvement of amino groups in the formation of COFs makes the unsuitable distribution of multiple amino groups in the monomer go against the connection of building blocks into the predicted topology,[22,23] leading to the difficult *de novo* synthesis of crystalline 3D COF-NH_2. To the best of our knowledge, no imine-linked 3D COF-NH_2 has been prepared so far.

Herein, we show the preparation of the first 3D COF-NH_2 (named JNU-5) *via* building block exchange (BBE) as a SP for GC separation of isomers. The direct condensation of 4-[tris(4-formylphenyl)methyl]benzaldehyde (TFPM) and 3,3′-diaminobenzidine (BD-NH_2) gave an amorphous polymer due to unsuitable distribution of multiple amino groups in BD-NH_2 (Fig. S1, ESI†). The BBE approach has already been proved to be attractive in the preparation of inaccessible *de novo* materials.[24,25] Therefore, JNU-5 was synthesized *via* the exchange of *p*-phenylenediamine (PA) in the parent 3D COF TFPM-PA with BD-NH_2 (Fig. 1). The longer BD-NH_2 than PA would not only introduce the amino group to the 3D COFs, but also bring an evident change in the powder X-ray diffraction (PXRD) peak after the BBE, which can efficiently identify the BBE process.

The crystallization of COFs is a thermodynamically controlled self-healing process.[4,26] So the BBE conditions including the content of BD-NH_2, reaction time and reaction temperature were studied in detail to obtain highly crystalline JNU-5. The results showed that the newly formed crystalline JNU-5 was obtained *via* the reaction of 10 equivalent (equiv.) of BD-NH_2 and TFPM-PA at 90 °C for 3 days (Fig. S1–S4, ESI†).

[a] *State Key Laboratory of Food Science and Technology, Jiangnan University, Wuxi, 214122, China. E-mail: hlqian@jiangnan.edu.cn*
[b] *Guangdong Laboratory for Lingnan Modern Agriculture, Guangzhou, 510642, China*
[c] *Institute of Analytical Food Safety, School of Food Science and Technology, Jiangnan University, Wuxi, 214122, China*
[d] *Key Laboratory of Synthetic and Biological Colloids, Ministry of Education, Jiangnan University, Wuxi, 214122, China*

† Electronic supplementary information (ESI) available: Methods, additional figures (Fig. S1–S24) and tables (Tables S1–S7). See DOI: https://doi.org/10.1039/d2cc02383k

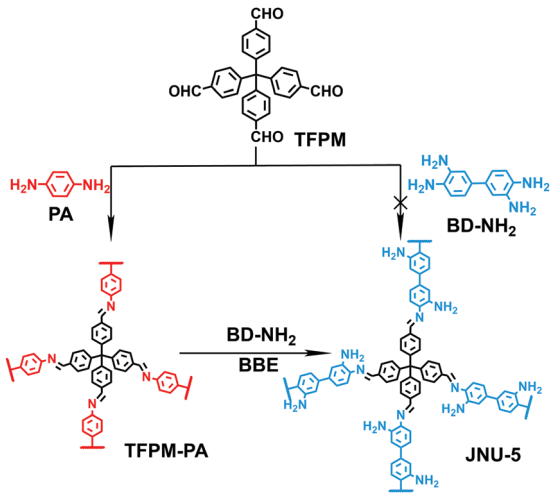

Fig. 1 Design and preparation of 3D COF-NH_2 (JNU-5) *via* BBE.

The successful preparation of JNU-5 *via* BBE was first verified by Fourier transform infrared (FTIR) spectroscopy. The appearance of an imine peak in the FTIR spectrum of the parent COF TFPM-PA confirmed the successful Schiff-base reaction of TFPM and PA (Fig. S5, ESI†). In contrast, the obtained JNU-5 not only gave new vibration bands of amino groups at 3232–3459 cm^{-1} and imine at 1637 cm^{-1}, but also lacked the aldehyde peaks of TFPM (Fig. 2a and Fig. S6, ESI†). The evident different peak positions of amino groups in the FTIR spectra of JNU-5 and BD-NH_2 indicate that the amino group of JNU-5 is not caused by the residues of BD-NH_2 (Fig. S6, ESI†), confirming the preparation of JNU-5.

To further provide complementary evidence of the BBE process, ^{13}C solid-state nuclear magnetic resonance (SNMR) spectroscopy was performed to characterize the specific groups of TFPM-PA and JNU-5. The carbon peak of the imine bond at 157 ppm confirmed the formation of imine linkage in TFPM-PA (Fig. S7, ESI†). In contrast, JNU-5 gave more carbon peaks in the ^{13}C SNMR spectra. The extra carbon peaks at 114 and 140 ppm were assigned to the carbon of biphenyl (Fig. 2b and Fig. S8, ESI†). The carbon signal for aromatic amines at 144 ppm also indicates the successful BBE of PA in TFPM-PA with BD-NH_2 (Fig. S8, ESI†).

PXRD provided strong evidence for the BBE process because the different lengths of BD-NH_2 and Pa would lead to obtaining different PXRD patterns of COFs. The parent COF TFPM-PA exhibited a main characteristic PXRD peak at 7.31°, matching with the reported PXRD position (Fig. 2c).[27] After BBE with BD-NH_2, the main PXRD peak of the obtained JNU-5 obviously changed from 7.31° to 6.59°, proving the successful BBE process and the crystallinity of JNU-5.

To resolve the specific structure of JNU-5, the computational simulation in conjunction with the PXRD analysis was performed. The building units of tetrahedral TFPM and linear BD-NH_2 indicate the feasible diamond structure of JNU-5.[6,28,29] Therefore, a series of simulated structures for JNU-5 with 5, 7, 9, and 11-fold-interpenetrated diamond nets (dia-5, 7, 9, and 11) were built to obtain the simulated PXRD patterns. Comparison of the simulated and experimental PXRD patterns reveals that dia-9 matches well with the structure of JNU-5 (Fig. S9, ESI†). The refinement further gave a more precise unit cell of JNU-5 (space group $I41/A$, $a = b = 26.8148$ Å, $c = 8.1893$ Å, and $\alpha = \beta = \gamma = 90°$) with $R_{wp} = 5.23\%$ and $R_p = 4.04\%$ (Table S1, ESI† Fig. 2d and 3).

The porosity of JNU-5 was evaluated with the N_2 adsorption–desorption experiment. TFPM-PA gave a BET surface area of 565 $m^2\ g^{-1}$, a pore size of *ca.* 9.3 Å and a pore volume of 3.6 $cm^3\ g^{-1}$. The introduction of amino groups resulted in little decrease of the BET surface area (419 $m^2\ g^{-1}$) and pore volume (2.8 $cm^3\ g^{-1}$) of JNU-5, whereas the replacement of PA with longer BD-NH_2 led to the increase of pore size for JNU-5 (*ca.* 13.0 Å) (Fig. S10 and S11, ESI†). The scanning electron microscopy (SEM) image shows that the cluster-like TFPM-PA obviously changed to sphere-like morphology after BBE (Fig. S12 and S13, ESI†). The thermogravimetric analysis of TFPM-PA

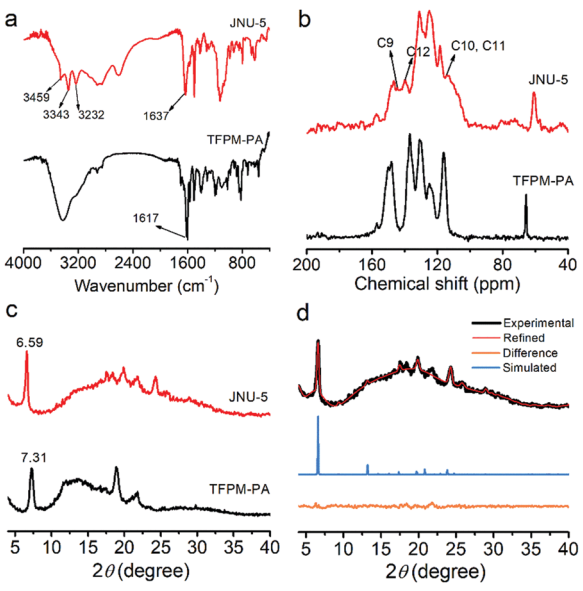

Fig. 2 (a) PXRD patterns, (b) FTIR spectra, and (c) ^{13}C SNMR spectra of the prepared 3D COFs before and after BBE. (d) Experimental, simulated, and refined PXRD patterns of JNU-5 and the difference between the experimental and refined PXRD patterns.

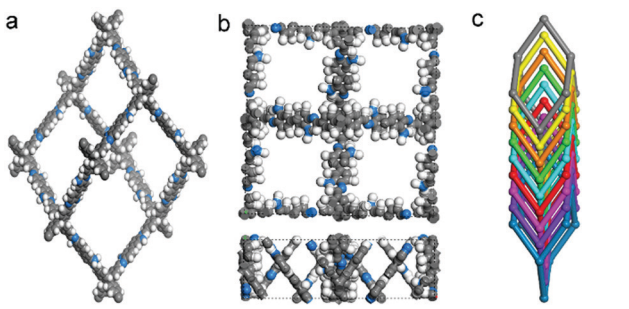

Fig. 3 (a) Space-filling model of the single diamond structure of JNU-5. (b) Top and side views of refined unit cell of JNU-5. (c) Structural representation of dia-9 topology.

and JNU-5 provided evidence for sufficient thermal stability of the prepared 3D COFs for their subsequent application in GC (Fig. S14, ESI†).

The highly thermally stable porous aromatic structure and rich amino group make JNU-5 promising as an SP for GC. The JNU-5-capillary was prepared *via* an *in situ* growth approach. Since the crystallinity of JNU-5 on the surface of capillary cannot be characterized directly, we prepared the JNU-5 bonded fused-silica plate (JNU-5-plate) in the same way as JNU-5-capillary. Similar PXRD patterns of JNU-5 powder and JNU-5-plate indirectly verified the crystallinity of the bonded JNU-5 on the capillary (Fig. S15, ESI†). Besides, JNU-5-capillary gave both the FTIR peaks of silica capillary and JNU-5, further proving the successful covalent growth of JNU-5 (Fig. S16, ESI†). In contrast to bare capillary, JNU-5-capillary showed evident distribution of the JNU-5 particles on the capillary wall (Fig. S17 and S18, ESI†). The successful preparation of TFPM-PA covalently bonded capillary (TFPM-PA-capillary) was also confirmed in the same way as for JNU-5-capillary (Fig. S19–S21, ESI†).

As one of word-changing separation,[14] the separation of the xylene isomers was first performed on the JNU-5-capillary. All the four isomers were successfully resolved, and excellent baseline separation (resolution of 1.85 to 2.89) with high column efficiency (11 429 plates m^{-1} for *m*-dichlorobenzene) was achieved on JNU-5-capillary under a constant temperature in 3.5 min (Fig. 4a and Table S2, ESI†). The elution sequence of xylene isomers indicates that the separation is not based on the boiling point.

To figure out the active sites for the separation of xylene isomers on JNU-5-capillary, the TFPM-BD with a similar structure to JNU-5 but no amino group was also applied as the SP for GC for comparison. No baseline separation of xylene isomers was realized with the TFPM-BD-capillary, TFPM-PA-capillary and amino functionalized capillary (APTES-capillary), indicating the key roles of the amino group and 3D COF structure for the separation (Fig. S22, ESI†). The pore size of JNU-5 (*ca.* 13.0 Å) is larger than the kinetic diameter of ethylbenzene (6.7 Å), *o*-xylene (7.4 Å), *m*-xylene (7.1 Å) and *p*-xylene (6.7 Å),[13] indicating the weak size exclusive effect on the separation.

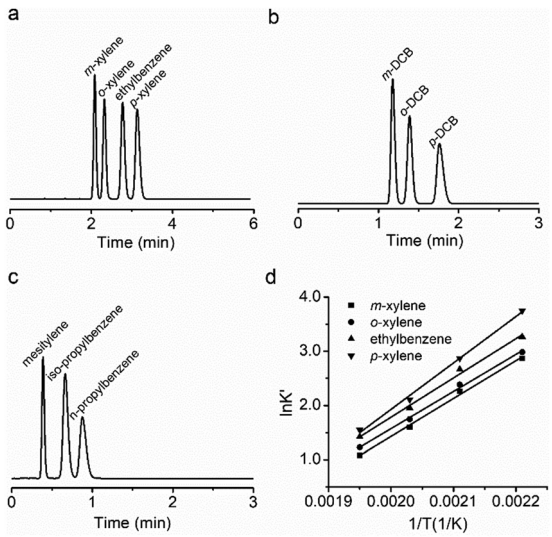

Fig. 4 GC chromatograms of (a) xylene isomers at 70 cm s^{-1} of N_2 (240 °C), (b) dichlorobenzene isomers at 120 cm s^{-1} of N_2 (260 °C), and (c) propylbenzene isomers at 320 cm s^{-1} of N_2 (260 °C) on JNU-5-capillary (10 m long × 0.53 mm i.d.). (d) Van't Hoff plots for the gas chromatographic separation of xylene isomers on JNU-5-capillary.

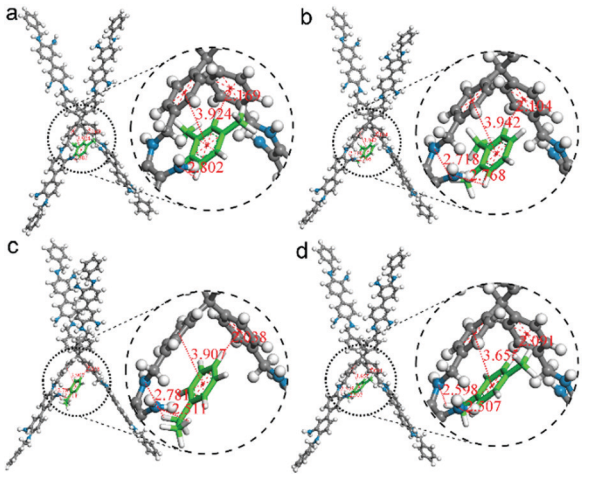

Fig. 5 Representative conformations of (a) JNU-5-*m*-xylene, (b) JNU-5-*o*-xylene, (c) JNU-5-ethylbenzene and (d) JNU-5-*p*-xylene obtained from the molecular docking with the lowest binding energy (distance Å). The COFs and isomers are shown in the ball-and-stick model (C grey, N blue and H white) and stick model (C green and H white), respectively.

Molecular docking was performed to obtain the most feasible conformation and interactions of xylene isomer interacted JNU-5 (JNU-5-EX).[25,30] All the xylene isomers in JNU-5-EX interacted with the amino group of JNU-5 (Fig. 5), proving the dominant role of amino groups in the separation. The molecular distance of JNU-5-EX further indicates that the involved interactions for the separation of xylene isomers are hydrogen bonding, π–π and C–H···π interactions (Fig. 5). Furthermore, the number and distance of the interactions demonstrate that the binding strength of xylene isomers on JNU-5 follows the order of *m*-xylene < *o*-xylene < ethylbenzene < *p*-xylene, which matched well with their elution order (Table S3, ESI†).

The enthalpy change (ΔH), the entropy change (ΔS), and the Gibbs free energy change (ΔG) were measured to better understand the separation mechanism of the xylene isomers using JNU-5-capillary (Fig. 4d and Table S4, ESI†). The negative ΔG implies that the separation of xylene isomers occurred spontaneously with JNU-5. The negative ΔH and ΔS further indicate that the separation is an exothermic and enthalpy-driven process. Moreover, the decrease of entropy suggests that xylene isomers lose freedom and become ordered on the SP of JNU-5 (Table S4, ESI†).

JNU-5-capillary is also good enough for the separation of other important intermediate raw isomers in petrochemistry. For instant, dichlorobenzene (*o*-DCB, *p*-DCB, and *m*-DCB) and propylbenzene isomers (*n*-propylbenzene, *iso*-propylbenzene and mesitylene) were baseline separated using JNU-5-capillary with a resolution of 1.64–3.18 and an efficiency of 572–11 429 plates m^{-1} (Fig. 4b and c). Moreover, the excellent baseline

separation of BTEX (benzene, toluene, ethylbenzene, and xylene isomers), *n*-alkanes, homologues of benzene and *n*-alcohols indicates the high potential of the JNU-5-capillary for the analysis of volatile organic compounds (Fig. S23, ESI†).

JNU-5-capillary was also compared with other capillary columns for the separation of isomers. The broad-spectrum commercial DB-5 capillary (10 m long × 0.53 mm i.d.) gave much lower separation performance for the isomers than JNU-5-capillary (Fig. S24, Table S5 and S6, ESI†). Even the general validated capillary column for the separation of xylene isomers (commercial HP-FFAP-capillary) with the same column size as that of JNU-5-capillary (10 m long × 0.53 mm i.d.) cannot offer baseline separation of xylene isomers as well (Fig. S25, Table S5 and S6, ESI†).

Although the higher binding strength led to longer separation time of xylene isomers with JNU-5 than MOF MIL-101,[15] JNU-5 still showed higher capability for the separation of isomers than lot of reported novel SPs. In fact, no baseline GC separation of xylene isomers was achieved with microporous organic polymers,[31] graphene quantum dots,[32] 2D COF BtaMth,[10] MOF-CJ3,[33] zeolitic metal azolate framework MAF-6,[13] and MOF UiO-66,[34] indicating the high potential of JNU-5 as the SP for GC separation of isomers.

The repeatability and stability of JNU-5-capillary were investigated with xylene isomers as model analytes. The relative standard deviation (RSD) of the retention time for run to run (n = 8) and day to day (n = 8) were 0.12–0.33% and 1.45–2.00% (Table S7, ESI†), respectively, indicating the stable separation performance of JNU-5-capillary. In order to evaluate the stability, JNU-5-capillary was aged by several runs of programmed temperature (40 °C to 350 °C at 2 °C min^{-1}). No obvious change in the GC chromatograms and in the RSD of 0.86–1.12% for the capillary factors (k) of xylene isomers (Fig. S26 and Table S8, ESI†) implies the good stability of the JNU-5-capillary. Moreover, the SEM and FTIR images of JNU-5-capillary further confirmed the structural stability of JNU-5 (Fig. S27, ESI†).

In summary, we have shown the first example of preparation of 3D COF-NH_2 (JNU-5) *via* BBE as the SP for GC separation of isomers. The high concentration of BD-NH_2 drives the replacement of PA in the parent 3D COF TFPM-PA to produce the daughter JNU-5 with a 9-fold-interpenetrated diamond net. The subsequently prepared JNU-5-capillary gave better GC resolution of aromatic isomers especially the xylene isomers than commercial capillary columns and many reported novel material-based capillary columns. The molecular docking confirmed the key role of the introduced amino group as well as the involvement of hydrogen bonding, π–π and C–H···π interactions in the promotion of the separation of isomers with JNU-5-capillary. This work enhances the performance of 3D COFs for GC as well as provides an efficient separation process for isomers.

We acknowledge the support from the Guangdong Laboratory for Lingnan Modern Agriculture Project (NZ2021037), the National Natural Science Foundation of China (No. 22076066 and 22176073), and the Program of ''Collaborative Innovation Center of Food Safety and Quality Control in Jiangsu Province''.

Conflicts of interest

There are no conflicts to declare.

Notes and references

1 H. M. El-Kaderi, J. R. Hunt, J. L. Mendoza-Cortes, A. P. Cote, R. E. Taylor, M. O'Keeffe and O. M. Yaghi, *Science*, 2007, **316**, 268–272.
2 Z. Wang, S. Zhang, Y. Chen, Z. Zhang and S. Ma, *Chem. Soc. Rev.*, 2020, **49**, 708–735.
3 H.-L. Qian, Y. Wang and X.-P. Yan, *TrAC, Trends Anal. Chem.*, 2022, **147**, 116516.
4 N. Huang, P. Wang and D. Jiang, *Nat. Rev. Mater.*, 2016, **1**, 16068.
5 S. Y. Ding and W. Wang, *Chem. Soc. Rev.*, 2013, **42**, 548–568.
6 X. Guan, F. Chen, Q. Fang and S. Qiu, *Chem. Soc. Rev.*, 2020, **49**, 1357–1384.
7 C. Yuan, W. Jia, Z. Yu, Y. Li, M. Zi, L.-M. Yuan and Y. Cui, *J. Am. Chem. Soc.*, 2022, **144**, 891–900.
8 H.-L. Qian, C.-X. Yang and X.-P. Yan, *Nat. Commun.*, 2016, **7**, 12104.
9 C.-X. Yang, C. Liu, Y. M. Cao and X.-P. Yan, *Chem. Commun.*, 2015, **51**, 12254–12257.
10 X. L. Huang, H. H. Lan, Y. L. Yan, G. Chen, Z. H. He, K. Zhang, S. L. Cai, S. R. Zheng, J. Fan and W. G. Zhang, *Sep. Sci. plus*, 2019, **2**, 120–128.
11 R. A. Meyers, *Handbook of petroleum refining processes*, McGraw-Hill Education, 2016.
12 Z. R. Herm, B. M. Wiers, J. A. Mason, J. M. V. Baten, M. R. Hudson, P. Zajdel, C. M. Brown, N. Masciocchi, R. Krishna and J. R. Long, *Science*, 2013, **340**, 960–964.
13 Y. Yang, P. Bai and X. Guo, *Ind. Eng. Chem. Res.*, 2017, **56**, 14725–14753.
14 D. S. Sholl and R. P. Lively, *Nature*, 2016, **532**, 435.
15 Z. Y. Gu and X. P. Yan, *Angew. Chem.*, 2010, **49**, 1477–1480.
16 C.-T. He, L. Jiang, Z.-M. Ye, R. Krishna, Z.-S. Zhong, P.-Q. Liao, J. Xu, G. Ouyang, J.-P. Zhang and X.-M. Chen, *J. Am. Chem. Soc.*, 2015, **137**, 7217–7223.
17 J.-H. Zhang, S.-M. Xie, L. Chen, B.-J. Wang, P.-G. He and L.-M. Yuan, *Anal. Chem.*, 2015, **87**, 7817–7824.
18 W. Q. Tang, J. Y. Xu and Z. Y. Gu, *Chem. – Asian J.*, 2019, **14**, 3462–3473.
19 P. Žuvela, M. Skoczylas, J. Jay Liu, T. Bączek, R. Kaliszan, M. W. Wong and B. Buszewski, *Chem. Rev.*, 2019, **119**, 3674–3729.
20 C. André, T. Gharbi and Y.-C. Guillaume, *J. Sep. Sci.*, 2009, **32**, 1757–1764.
21 J. Huang, X. Han, S. Yang, Y. Cao, C. Yuan, Y. Liu, J. Wang and Y. Cui, *J. Am. Chem. Soc.*, 2019, **141**, 8996–9003.
22 M. S. Lohse, T. Stassin, G. Naudin, S. Wuttke, R. Ameloot, D. De Vos, D. D. Medina and T. Bein, *Chem. Mater.*, 2016, **28**, 626–631.
23 H.-L. Qian, Y. Li and X.-P. Yan, *J. Mater. Chem. A*, 2018, **6**, 17307–17311.
24 P. Deria, J. E. Mondloch, O. Karagiaridi, W. Bury, J. T. Hupp and O. K. Farha, *Chem. Soc. Rev.*, 2014, **43**, 5896–5912.
25 H.-L. Qian, F.-L. Meng, C.-X. Yang and X.-P. Yan, *Angew. Chem.*, 2020, **59**, 17607–17613.
26 X. Feng, X. Ding and D. Jiang, *Chem. Soc. Rev.*, 2012, **41**, 6010–6022.
27 X. Guan, Y. Ma, H. Li, Y. Yusran, M. Xue, Q. Fang, Y. Yan, V. Valtchev and S. Qiu, *J. Am. Chem. Soc.*, 2018, **140**(13), 4494–4498.
28 F. J. Uribe-Romo, J. R. Hunt, H. Furukawa, C. Klöck, M. O'Keeffe and O. M. Yaghi, *J. Am. Chem. Soc.*, 2009, **131**, 4570–4571.
29 Y. B. Zhang, J. Su, H. Furukawa, Y. Yun, F. Gandara, A. Duong, X. Zou and O. M. Yaghi, *J. Am. Chem. Soc.*, 2013, **135**, 16336–16339.
30 G. M. Morris, R. Huey, W. Lindstrom, M. F. Sanner, R. K. Belew, D. S. Goodsell and A. J. Olson, *J. Comput. Chem.*, 2009, **30**, 2785–2791.
31 C. Lu, S. Liu, J. Xu, Y. Ding and G. Ouyang, *Anal. Chim. Acta*, 2016, **902**, 205–211.
32 X. Zhang, H. Ji, X. Zhang, Z. Wang and D. Xiao, *Anal. Methods*, 2015, **7**, 3229–3237.
33 Z. L. Fang, S. R. Zheng, J. B. Tan, S. L. Cai, J. Fan, X. Yan and W. G. Zhang, *J. Chromatogr. A*, 2013, **1285**, 132–138.
34 N. Chang and X. P. Yan, *J. Chromatogr. A*, 2012, **1257**, 116–124.

